



GLOBAL JOURNAL OF RESEARCHES IN ENGINEERING: A
MECHANICAL AND MECHANICS ENGINEERING
Volume 18 Issue 2 Version 1.0 Year 2018
Type: Double Blind Peer Reviewed International Research Journal
Publisher: Global Journals
Online ISSN:2249-4596 Print ISSN:0975-5861

Development of Local Diameter-Enlarged Processing Method by High-Frequency Induction-Heating Method

By Xia Zhu, Keiji Ogi & Nagatoshi Okabe
Ehime University

Abstract- In the present work, a new local hot working method is proposed to achieve a higher diameter-enlargement ratio and higher processing efficiency than those that can be obtained by cold working. Further, a high-frequency induction-heating device is built; this device is installed in a diameter-enlargement processing machine developed originally. A local diameter-enlargement part was formed by processing after being heated locally by the heating device, and its diameter-enlargement deformation behavior and its surface temperature were investigated experimentally. The diameter-enlargement ratio achieved with the proposed method was twice the diameter-enlargement ratio that can be achieved by cold working, with local heating for 120 s. This hot working method was effective for the diameter-enlargement forming process. The diameter-enlargement deformation behavior can be predicted approximately by a cycle parameter considering the effect of blue shortness.

Keywords: *diameter-enlargement ratio, heating time, surface temperature, local hot working, blue shortness.*

GJRE-A Classification: FOR Code: 091399



Strictly as per the compliance and regulations of:



© 2018. Xia Zhu, Keiji Ogi & Nagatoshi Okabe. This is a research/review paper, distributed under the terms of the Creative Commons Attribution-Noncommercial 3.0 Unported License (<http://creativecommons.org/licenses/by-nc/3.0/>), permitting all non commercial use, distribution, and reproduction in any medium, provided the original work is properly cited.

Development of Local Diameter-Enlarged Processing Method by High-Frequency Induction-Heating Method

Xia Zhu ^α, Keiji Ogi ^σ & Nagatoshi Okabe ^ρ

Abstract- In the present work, a new local hot working method is proposed to achieve a higher diameter-enlargement ratio and higher processing efficiency than those that can be obtained by cold working. Further, a high-frequency induction-heating device is built; this device is installed in a diameter-enlargement processing machine developed originally. A local diameter-enlargement part was formed by processing after being heated locally by the heating device, and its diameter-enlargement deformation behavior and its surface temperature were investigated experimentally. The diameter-enlargement ratio achieved with the proposed method was twice the diameter-enlargement ratio that can be achieved by cold working, with local heating for 120 s. This hot working method was effective for the diameter-enlargement forming process. The diameter-enlargement deformation behavior can be predicted approximately by a cycle parameter considering the effect of blue shortness.

Keywords: diameter-enlargement ratio, heating time, surface temperature, local hot working, blue shortness.

I. INTRODUCTION

Shafts having a larger local diameter than themselves are required in many mechanical parts, such as bearing stops and gear locations. A part with a large local diameter is called a “diameter-enlargement part.” Usually, cutting work or welding a fat ring on the shaft is used to work the part. However, these processing methods arise about the uselessness of the material for cutting work or the decrease of strength in the welded area. Thus, a new cold working method is proposed to enlarge the local diameter of a metal shaft by applying multiple loads of cyclic rotational bending stress and axial compressive stress normalized by the yield stress on the processed part [1-3]. In the processing method, the local diameter-enlargement part is formed easily under a load condition of low compressive stress at room temperature, so the uselessness of the material because of cutting work and the mechanical damage in the part caused by welding can be avoided. The influences of various processing conditions and the mechanical properties of the used

material on the diameter-enlargement behaviors are clarified, and a cycle parameter is proposed to evaluate the deformation behaviors under various processing conditions [4]. Further, the fatigue properties and safety against fatigue damage in the processed part are addressed [5-7]. However, only cold working has limitations regarding the processing efficiency and the maximum diameter-enlargement rate without fatigue damage generated in the foot of the processed part during the forming process. A large-scale processing machine is needed to improve the efficiency and the diameter-enlargement rate. Therefore, a new hot working diameter-enlargement processing method is proposed, in which the processed part is locally heated by a high-frequency induction-heating device and then formed by the processing method mentioned above. In the present research, a basic investigation is carried out to clarify the influence of the induction-heating conditions on the diameter-enlargement workability, and the diameter-enlargement rate and the processing efficiency obtained by the hot working are compared with those obtained by cold working.

II. EXPERIMENT

a) Experimental Equipment

Figure 1 shows an image diagram of a processing machine. The processing machine consists mainly of three components: (1) a component to set the bending angle, (2) component to load the axial-compressive force, and (3) an axial-rotary actuator. A test specimen was installed with an arbitrary distance between two holders by moving the parts loaded with an axial-compressive force. Fig. 2 shows a high-frequency induction-heating device to heat the processed part before forming starts.

b) Experimental method

A cold drawing S45C (Japanese Industrial Standard, JIS G4051-2009) round bar that was $D_0 = 32$ mm in diameter and $L_0 = 155$ mm in length was used as the test specimen. Table 1 presents the chemical composition of the material (mass %). Table 2 lists the mechanical properties of the sample material at room temperature.

Author ^α ^σ: Department of Mechanical Engineering, Faculty of Engineering, Ehime University, Matsuyama, Japan.
e-mails: zhu.xia.mx@ehime-u.ac.jp, ogi.keiji.mu@ehime-u.ac.jp

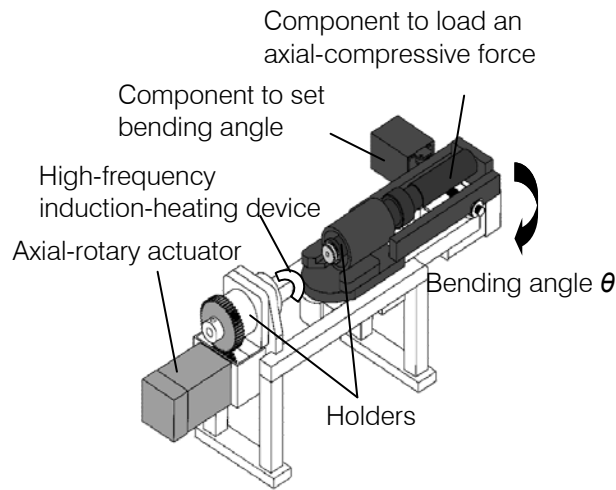


Figure 1: Image diagram of the processing machine

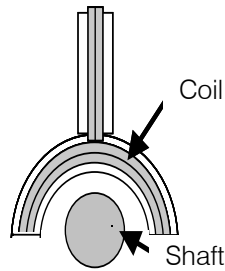


Figure 2: Schema of high-frequency induction-heating device

Table 1: Chemical compositions of S45C (mass)

| | C | Si | Mn | P | S |
|------|------|------|------|-------|-------|
| S45C | 0.43 | 0.21 | 0.61 | 0.011 | 0.006 |

In the high-frequency induction-heating experimental method, a test specimen was installed coaxially between two holders in the processing machine; the specimen was then rotated and locally heated by the high-frequency induction-heating device. At the end of the set heating time, the heating coil was removed. The distance between both holders at that point is defined as l_0 .

In the diameter-enlargement processing experimental method, the test specimen was loaded with an axial-compressive stress of σ_c / σ_y , which is an axial-compressive stress normalized by yield stress σ_y , in the axial-compressive side. The specimen was rotated with a rotational speed ω after the heating experiment ends. Then, it is loaded gradually to a set bending angle θ . Until the local diameter-enlargement part is formed on the test specimen and its diameter reaches the required diameter-enlargement rate D/D_0 , the values of θ , σ_c / σ_y , and ω are returned to zero.

An infrared thermometer and a laser Displacement meter, respectively, continuously measured the surface temperatures and changes in the distance l between both holders in the processed part.

Table 2: Mechanical properties of S45C at room temperature

| Young's modulus E (GPa) | Yield strength σ_y (MPa) | Tensile strength σ_B (MPa) | Reduction In area φ (%) |
|------------------------------|------------------------------------|--------------------------------------|---------------------------------------|
| 210 | 643 | 756 | 32.8 |

Table 3: Diameter-enlargement processing conditions

| | |
|--|--------------------|
| Normalized axial-compressive stress σ_c / σ_y | 0.95, 0.97, 1.0 |
| Bending angle θ (degree) | 3, 4, 5 |
| Rotating speed ω (rpm) | 40 |
| Final number of revolution N_{20} | 20 |
| Distance between two holder l_0 (mm) | 55 |

c) Experimental conditions

Constant heating conditions of 2.2 kW, 420 V, and 21.7 kHz were set by adjusting the voltage of the high-frequency power source. The heating times were 20 to 120 s. Table 3 presents the processing conditions. The processing conditions are the same as that used in the cold working method, to compare the different work abilities [8].

III. EXPERIMENTAL RESULTS AND DISCUSSION

a) Surface temperature change in both specimen and holder

Figure 3 shows the changes in the maximum surface temperature on the processed part as the high-frequency induction-heating time was increased. In addition, the abscissa shows the distance from the left holder in the processing machine. The surface temperature rises as the heating time increases. In the temperature distribution, the temperature rise is the fastest in the center section of the processed part, which is right under the coil, and the temperature rise range extends with the increase in the heating time. The temperature at the left holder end also rises with the increase in the heating time, as shown in Fig. 4. This suggests that thermal energy transfers from the processed part to the holders via heat conduction, and loss of energy is confirmed.

Figure 5 shows the various temperature changes in the processed part just after heating ends, just before processing starts, and just after processing ends. However, the maximum surface temperatures rose rapidly with the increase in the initial heating time period in all cases, and the rising slopes of the temperature become gradual with a heating time > 60 s. Moreover, as shown in the figure, the surface temperature at the start of processing was lower than that at the end of processing with a heating time < 50 s; however, the surface temperature at the start of processing was higher than that at the end of processing and maintained the high level with a heating time > 50 s. Under the conditions of a heating time > 50 s, the surface temperature rise was caused by a large plastic deformation advancing during the forming process, although thermal energy kept transferring to the atmosphere and the holder; thus, the heating was effective in promoting plastic deformation during the forming process. Moreover, the maximum surface temperature just before the beginning of processing decreased between 100 K and 200 K, compared with the temperature just after heating ended. Thus, it is necessary to consider the temperature decrease caused by the loss of thermal energy until the processing starts when setting the heating time or the heating temperature. Moreover, blue shortness is a brittle characteristic of steel involving the increase in tensile strength and hardness, decrease in percentage elongation, and percentage reduction in area at a temperature of 473 K to 573 K [9-10].

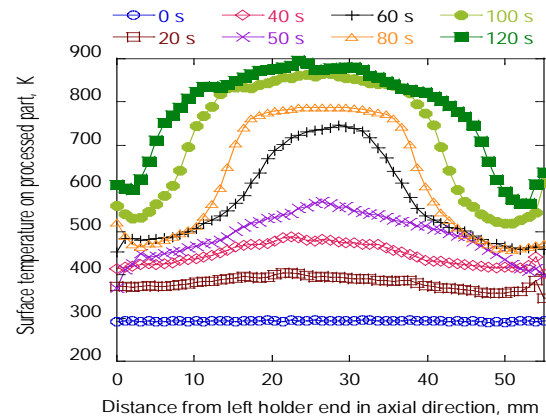


Figure 3: Changes in surface temperature distribution with increase in heating time

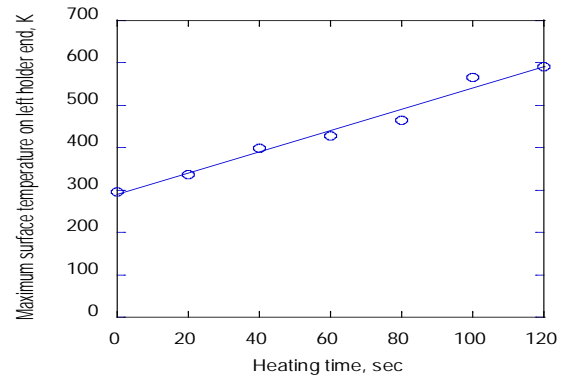


Figure 4: Changes in the maximum surface temperature on left holder end with the increase in heating time

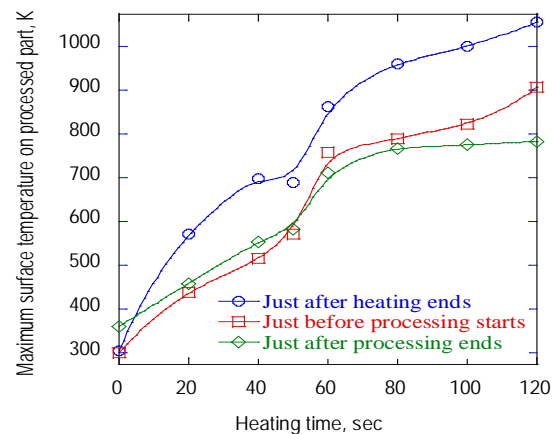


Figure 5: Changes in the maximum surface temperature on the processed part with the increase in heating time ($\theta = 3^\circ$, $\sigma_o/\sigma_y = 0.97$, $N = 20$)

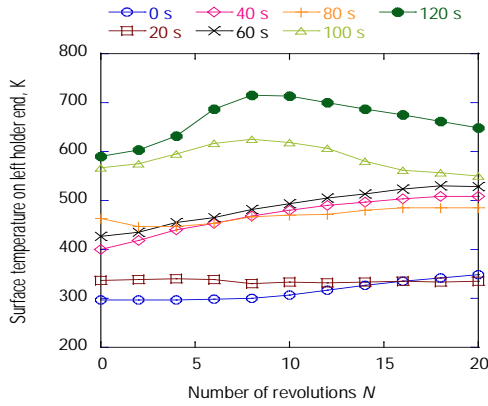


Figure 6: Changes in maximum surface temperature on the left holder end with the increase in number of revolutions in each heating time ($\theta = 3^\circ$, $\sigma_c / \sigma_y = 0.97$)

Figure 6 shows that the maximum surface temperature at the left holder end changed with an increase in the number of revolutions for each heating time under the conditions of $\theta = 3^\circ$ and $\sigma_c / \sigma_y = 0.97$, and the Temperature passed into the blue shortness temperature range during the forming process, with a heating time of 40–100 s. However, Fig. 7 shows that the maximum surface temperature on the processed part passed into the blue shortness temperature range during the forming process with a heating time of 40–50 s. Thus, it is necessary to set heating conditions such that blue shortness is not generated in the test specimen and holder.

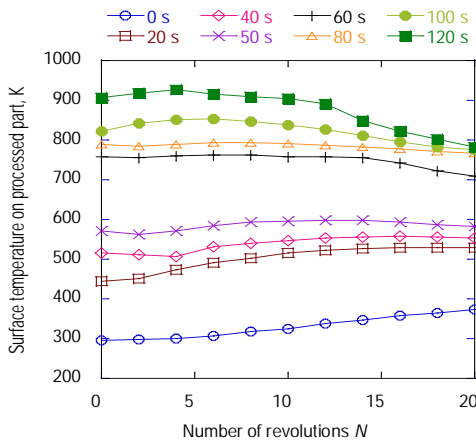


Figure 7: Change in maximum surface temperature on the processed part with the increase in number of revolutions in each heating time ($\theta = 3^\circ$, $\sigma_c / \sigma_y = 0.97$)

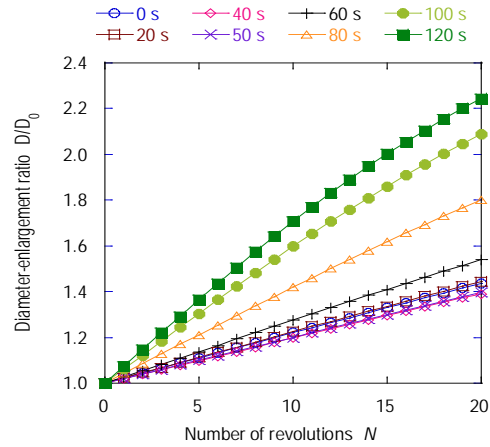


Figure 8: Diameter-enlargement deformation behaviors with increase in number of revolutions in each heating time ($\theta = 3^\circ$, $\sigma_c / \sigma_y = 0.97$)



(a) Heating time = 0 sec (b) Heating time = 40 sec (c) Heating time = 120 sec

Figure 9: Photograph in part processed at heating time = 0 sec (cold working), 40 sec and 120 sec

b) Influence of heating time on diameter-enlargement deformation behavior

Figure 8 shows the behavior of the diameter-enlargement rate D/D_0 with an increase in the number of revolutions N for each heating time. At a heating time of 20–50 s, the D_{20}/D_0 value at $N = 20$ with hot working was lower than that with cold working (heating time = 0) because of blue shortness, and the results shown in Fig. 8 agree well with the result shown in Fig. 7. However, at a heating time > 50 s, a heating effect appeared in the diameter-enlargement deformation behavior compared with that obtained by cold working, and the slopes of D/D_0 increased rapidly with the increase in heating time. The D_{20}/D_0 obtained by hot working at a heating time of 120 s is significantly higher than that obtained by cold working; the D_{20}/D_0 value reached 2.25. Fig. 9 shows the test specimens heated under the different heating conditions with a heating time of 0 s (cold working), 40 s, and 120 s, but under the same processing conditions of $\theta = 3^\circ$, $\sigma_c / \sigma_y = 0.97$, $N = 20$. It was confirmed experimentally that heating is effective for the progress of diameter-enlargement deformation progress at a heating time of > 50 s.

c) Formula for diameter-enlargement deformation behavior

Based on previous studies (6), the axial compression rate l/l_0 , which is the change in the distance between both holders and the diameter-enlargement rate D/D_0 in the processed part can be expressed, respectively, by Eqs. (1) and (2).

$$l/l_0 = \exp\{\varepsilon_{p0} \{1 - \exp(-N/N_0)\}\} \quad (1)$$

$$D/D_0 = [\exp\{\varepsilon_{p0} \{\exp(-N/N_0) - 1\}\}]^{1/2} \quad (2)$$

Where ε_{p0} is the maximum average axial-plastic strain, which is approximately 3.0 except for the blue shortness temperature range. N_0 is a cycle parameter that can evaluate uniformly the processing conditions and can be calculated from the relation of $D/D_0 - N$ or $l/l_0 - N$ obtained through the processing experiments. The relation between N_0 and the normalized axial-compressive stress σ_c/σ_y in each bending angle θ is shown in Fig. 10 and is expressed by Eq. (3). Then, the relation between coefficients N_0^* , α , and the bending angle θ is shown in Fig. 11 and is expressed by Eqs. (4) and (5).

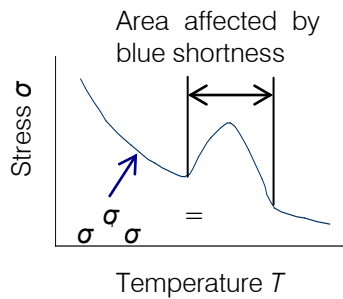
$$N_0 = N_0^* / (\sigma_c / \sigma_y)^\alpha \quad (3)$$

$$N_0^* = \hat{N}_0^* \theta^m \quad (4)$$

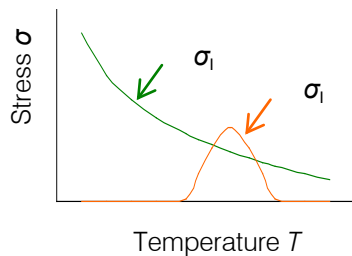
$$\alpha = \alpha_0 \theta^m \quad (5)$$

Table 4: Material constants included in Eq. (6)

| \hat{N}_0^* | α_0^* | m |
|---------------|--------------|-------|
| 50 | 73 | -0.75 |



(a) Conceptual diagram



(b) Decomposition diagram

Figure 12: Relation between stress and temperature

Table 5: Material constants included in Eqs. (7)- (8)

| β_0 | 2.56×10^{-3} | $\beta_1 \text{ (K}^{-1}\text{)}$ | -2.82×10^{-7} |
|---------------------|-----------------------|-----------------------------------|------------------------|
| $K_0 \text{ (MPa)}$ | 1.86×10^3 | $K_1 \text{ (MPa/K)}$ | -1.11 |
| n_0 | 1.94×10^{-1} | $n_1 \text{ (K}^{-1}\text{)}$ | -4.40×10^{-5} |
| $C_1 \text{ (MPa)}$ | 6.90×10^2 | $C_2 \text{ (K}^{-2}\text{)}$ | -9.88×10^{-5} |
| C_3 | 5.04×10^{-1} | $T_0 \text{ (K)}$ | 537 |

The relation between N_0 and the processing conditions of normalized axial-compressive stress σ_c/σ_y and bending angle θ is expressed by Eq. (6), obtained by substituting Eq. (4) and Eq. (5) in Eq. (3). Because N_0 is large, the processing requires more revolutions.

$$N_0 = \hat{N}_0^* \theta^m / (\sigma_c / \sigma_y)^{\alpha_0^* \theta^m} \quad (6)$$

The material constants included in Eq. (6) are listed in Table 4. However, the relation (8) between the stress σ of the sample material and the temperature T is shown in Fig. 12. Fig. 12(a) shows that the stress rises rapidly according to the increase in work hardening in the blue shortness temperature range. The relation between stress and temperature can be expressed by the sum of two stress components σ_1 and σ_{11} , as shown in Fig. 12(b). That is, σ_1 decreases monotonously for a temperature rise without the effect of blue shortness, and it is a stress component with the usual temperature dependency. Moreover, σ_{11} shows a stress component that increases according to blue shortness. The relation between stress σ and plastic strain ε_p in the total temperature range, including the blue shortness range, is shown in Eq. (7).

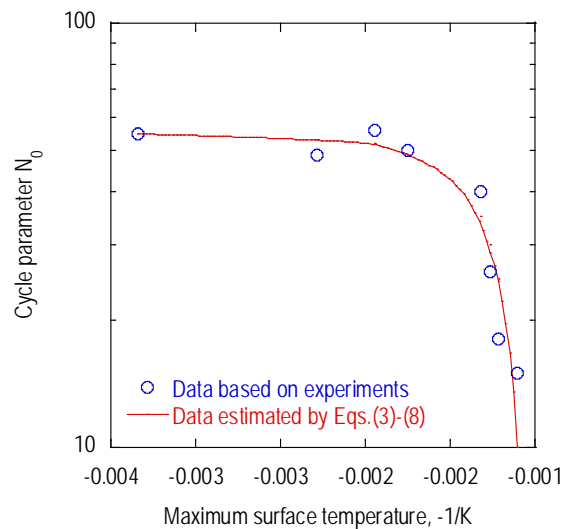


Figure 13: Relationship between cycle parameter and the maximum surface temperature just before processing starts

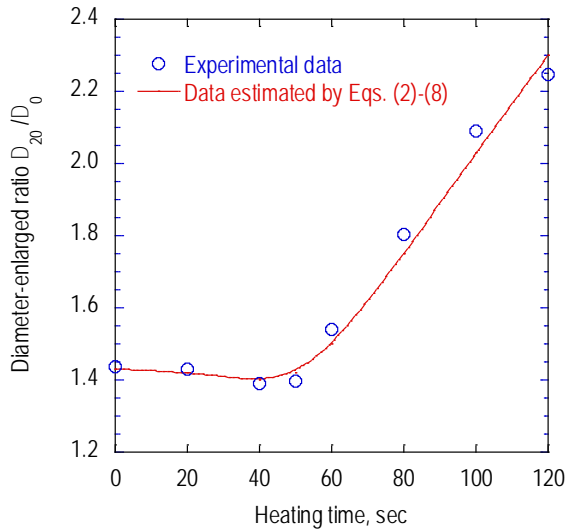


Figure 14: Changes of diameter-enlargement rate at number of revolution $N=20$ with the increase in heating time

$$\sigma = K(\epsilon_p + \beta)^n + C_1 \exp\{C_2(T - T_0)^2\} \epsilon_p^{C_3} \quad (7)$$

where β is the yield strain. The material constants K , β , and n included in Eq. (7) change linearly with temperature and are shown in Eqs. (8) – (10).

$$\beta = \beta_0 + \beta_1 T \quad (8)$$

$$K = K_0 + K_1 T \quad (9)$$

$$n = n_0 + n_1 T \quad (10)$$

The material constants included in Eqs. (7) - (8) are listed in Table 5. Figure 13 shows relation between N_0 and the maximum surface temperature just before processing starts. In the figure, the symbol O represents data obtained through the processing experiments, and the curve shows data estimated by Eqs. (3) – (8); the N_0 estimated is in close agreement with the experiment data in all temperature ranges. Then, the curve (Fig. 14), which shows the relation between the diameter-enlargement rate D_{20}/D_0 estimated by Eqs. (2) – (10) and heating time, is in good agreement with the experimental data.

IV. CONCLUSION

In this research, diameter-enlargement processing experiments were conducted after locally heating the specimen with a high-frequency induction heating device installed in a diameter-enlargement processing machine. The heating conditions were clarified for achieving a higher diameter-enlargement rate and higher processing efficiency than those obtained by cold working. The main results obtained are as follows.

1. The diameter-enlargement rate obtained by hot working was more than twice that obtained by cold working. This rate is achieved by local high-frequency induction heating in just 120 s, which shows that hot working is effective for the diameter-enlargement forming process.
2. It is necessary to avoid heating in the temperature range of 473 K-573 K, because the diameter-enlargement rate and the processing efficiency decrease due to the generation of blue shortness.
3. Diameter-enlargement deformation behavior can be estimated approximately by the cycle parameter, which is considered the effect of blue shortness.

ACKNOWLEDGMENTS

The present authors would like to thank Neturen Co., Ltd. (<http://www.k-neturen.co.jp/>) for providing a processing machine, and the authors also thank Ph. D. in Eng. K. Mori for his support.

The authors would like to thank Editage (www.editage.jp) for English language editing.

REFERENCES RÉFÉRENCES REFERENCIAS

1. T. Iura, N. Okabe, X. Zhu, and K. Mori, "A New Cold Working with Local Superplastic Deformation for a Metal Bar " Proceedings of the 7th International Conference on Technology of Plasticity, Vol.1 , pp.493-498, 2002.
2. T. Iura, N. Okabe and X. Zhu, "Development of Novel Plastic Working Process for Producing a Collar on a Round Shaft Journal of the Japan Society Technology Plasticity", Vol.44, No.514, pp.45-49, 2003.
3. T. Iura, N. Okabe and X. Zhu, "Influence of Strength Properties on Diameter Increase for Processed Material during the Process of Enlarging a Partial Diameter", Journal of the Japan Society Technology Plasticity, Vol.46, No.531, pp.55-59, 2005.
4. N. Okabe, X. Zhu, K. Mori and T. Iura, "Application of Processing Method to Enlargement of Diameter of Hollow Round Bar as Shaft", Journal of the Japan Society Technology Plasticity, Vol.46, No.533, pp.90-94, 2005.
5. T. Iura, N. Okabe, and X. Zhu, "Fatigue Properties and Fatigue Damage in a Round Shaft with a Collar Formed by a Novel Processing Method for Enlarging Diameter", Journal of the Japan Society Technology Plasticity, Vol.45, No.516, pp. 35-39, 2004.
6. X. Zhu, N. Okabe, K. Ogi, M. Takahashi, "Fatigue Strength of Shaft with Diameter Enlarged Partially by Cyclic Bending and Axial Compressive Loading", Appl. Mech. Mater., Vols. 217-219, pp. 2346-2350, 2012.

7. The diameter- ahashi, K. Ogi, M. Takahashi, N. Okabe, "Investigation of Crack Generation in a Notch during Diameter-Enlargement Working Method Processing", Key Eng. Mater., Vol. 656-657, pp. 473-478, 2015.
8. N. Okabe, X. Zhu, K. Mori and T. Iura, "Application of the Processing Method for Enlarging Partial Diameter to Shaft for Practical Use", Journal of the Japan Society Technology Plasticity, Vol.47, No.540, pp.49-53, 2006.
9. Japan Institute of Invention and Innovation Japanese BLAC to the OECD Corp., Metal heat treatment, 2006.
10. H. Tachiya, T. Aramoto, K. Takagi, A. Hojo and A. Chatani, "Temperature Dependent Constitutive Equation for Carbon Steels with Consideration of Blue Brittleness", Journal of the Japan Society of Mechanical Engineers (volume A), Vol.71, No.703, pp.435-442, 2006.

